

Basicity of bisperhalophenyl aurates toward closed-shell metal ions: metallophilicity and additional interactions

José M. López-de-Luzuriaga · Miguel Monge ·
M. Elena Olmos · María Rodríguez-Castillo ·
Antonio Laguna · Fernando Mendizabal

Received: 22 October 2010 / Accepted: 1 February 2011 / Published online: 19 February 2011
© Springer-Verlag 2011

Abstract The interaction of bisperhalophenyl aurates $[\text{AuR}_2]^-$ ($\text{R} = \text{C}_6\text{F}_5$, $\text{C}_6\text{F}_3\text{Cl}_2$, and C_6Cl_5) with the closed-shell Ag^+ , Cu^+ , and Tl^+ ions has been studied theoretically and compared with the experimentally known X-ray diffraction crystal structures. Initially, the aurates have been fully optimized at MP2 level of theory in a D_{2h} symmetry. The analysis of the basicity of the three aurates $[\text{AuR}_2]^-$ ($\text{R} = \text{C}_6\text{F}_5$, $\text{C}_6\text{F}_3\text{Cl}_2$ and C_6Cl_5) against Ag^+ ions in a C_{2v} symmetry has been calculated in point-by-point bsse-corrected interaction energy analysis at HF and MP2 levels of theory. Taking into account the experimental observation of additional interactions between the heterometals and C_{ipso} atoms at the perhalophenyl rings or halogen atoms at the *ortho* position of the perhalophenyl rings, dinuclear models of the type $[\text{AuR}_2]^- \cdots \text{Ag}^+$ ($\text{R} = \text{C}_6\text{Cl}_5$, and C_6F_5); $[\text{AuR}_2]^- \cdots \text{Cu}^+$ ($\text{R} = \text{C}_6\text{F}_5$, and C_6Cl_5) and $[\text{AuR}_2]^- \cdots \text{Tl}^+$ ($\text{R} = \text{C}_6\text{F}_5$, and C_6Cl_5) with a C_{2v} , C_2 , and C_s symmetries

Dedicated to Professor Pekka Pyykkö on the occasion of his 70th birthday and published as part of the Pyykkö Festschrift Issue.

J. M. López-de-Luzuriaga (✉) · M. Monge (✉) ·
M. E. Olmos · M. Rodríguez-Castillo
Departamento de Química, Grupo de Síntesis Química
de La Rioja, UA-CSIC, Universidad de La Rioja,
Complejo Científico-Tecnológico, 26004 Logroño, Spain
e-mail: josemaria.lopez@unirioja.es

M. Monge
e-mail: miguel.monge@unirioja.es

A. Laguna
Departamento de Química Inorgánica, Instituto de Ciencia de
Materiales de Aragón, Universidad de Zaragoza-CSIC,
50009 Zaragoza, Spain

F. Mendizabal
Departamento de Química, Facultad de Ciencias,
Universidad de Chile, Casilla, 653 Santiago, Chile

have been optimized at DFT-B3LYP level. The interaction energies have been computed through bsse-corrected single point HF and MP2 calculations. The energy stabilization provided and the heterometal preference have been analyzed and compared with the experimental results.

Keywords Gold · Silver · Copper · Thallium · Metal–metal interactions

1 Introduction

Metallophilic bonding interactions between Au(I) and other closed-shell metals like Ag(I), Cu(I), Hg(II), Tl(I), Pb(II), etc., have been studied from both experimental [1] and theoretical [2–5] viewpoints regarding the intrinsic nature of the interaction and in many cases the photophysical properties associated with them [6, 7]. In the last years, we have used basic aurates such as $[\text{AuR}_2]^-$ ($\text{R} = \text{C}_6\text{F}_5$, $\text{C}_6\text{F}_3\text{Cl}_2$ and C_6Cl_5) that react with Lewis acid metal salts allowing the isolation of complexes bearing unsupported Au(I)···M interactions (M = Ag(I) [8–10], Cu(I) [11, 12], Tl(I) [13–18], and Bi(III) [19]). Ab initio calculations at density functional theory (DFT), Hartree–Fock (HF) and at second-order Møller–Plesset perturbation theory (MP2) levels have permitted the analysis of the nature of these interactions showing a strong ionic character (ca. 80–85% of the interaction) and an additional dispersion-type component (ca. 15–20%) when correlation effects are included in the calculations. The strong stabilization obtained through the formation of these metallophilic interactions (around 250–300 kJ mol⁻¹) has allowed to stabilize many types of structural arrangements as, for instance, Au(I)-Tl(I) loosely bound butterfly clusters (a) [15]; Au(I)-Tl(I) infinite linear (b) [14] or zigzag chains [13, 16, 17];

$\text{Au}_2(\text{I})\text{--Ag}_2(\text{I})$ tetranuclear units linked through aurophilic interactions (c) [8–10]; a $\text{Au}(\text{I})\text{--Ag}_4(\text{I})$ square pyramidal disposition in which two anionic fragments attract each other (d) [20] or polymeric $\text{Cu}(\text{I})$ -pyrimidine chains displaying unsupported $\text{Au}(\text{I})\cdots\text{Cu}(\text{I})$ interactions at each copper site (e) [11] (see Scheme 1).

A deeper analysis of the experimental X-ray structures of many of these heterometallic $[\text{AuR}_2]^- \cdots \text{M}^{n+}$ systems permits to observe a common trend, which is the concomitant presence of heterometallic $\text{Au}(\text{I})\cdots\text{M}$ closed-shell interactions with weaker $\text{M}\cdots\text{C}_{ipso}$ (C_{ipso} = ipso carbon from the perhalophenyl rings bonded to gold) and/or $\text{M}\cdots\text{X}$ (X = halogen atom in *ortho* position of the perhalophenyl rings) interactions, depending on the heterometal and on the pentahalophenyl rings (See Table 1). We have theoretically accounted previously for the $\text{M}\cdots\text{C}_{ipso}$ weak interactions in the study of the $\text{Au}(\text{I})\text{--Ag}_4(\text{I})$ square pyramidal case [20] or in the calculations performed on $[\text{Au}(\text{C}_6\text{F}_5)(\text{ylide})]\cdots[\text{Ag}_2(\text{CF}_3\text{CO}_2)_2]$ [21] systems showing an additional stabilization through two $\text{C}_{ipso}\cdots\text{Ag}$ interactions of 21 kJ mol^{-1} , in the first case, and one $\text{C}_{ipso}\cdots\text{Ag}$ interaction of 37 kJ mol^{-1} in the second one. From an experimental viewpoint, the presence of $\text{M}\cdots\text{C}_{ipso}$ interactions is always observed when $\text{M} = \text{Ag}^+$ or Cu^+ and $\text{R} = \text{C}_6\text{F}_5$ or $\text{C}_6\text{F}_3\text{Cl}_2$ (no structural data available for C_6Cl_5) and to a lesser extent when $\text{M} = \text{Ti}^+$, while the $\text{M}\cdots\text{X}_{ortho}$ interactions are widely observed for $\text{M} = \text{Ti}^+$ and $\text{R} = \text{C}_6\text{Cl}_5$, C_6F_5 , or $\text{C}_6\text{F}_3\text{Cl}_2$, but not observed for $\text{M} = \text{Ag}^+$ or Cu^+ and $\text{R} = \text{C}_6\text{F}_5$ or $\text{C}_6\text{F}_3\text{Cl}_2$. Since the $\text{M}\cdots\text{C}_{ipso}$ and $\text{M}\cdots\text{X}_{ortho}$ distance also depends on the $\text{Au}\cdots\text{M}$ distance, it seems that a larger size of the heterometal (Ti) and the halogen in *ortho* position (Cl) favors the $\text{M}\cdots\text{X}$ interaction rather than the $\text{M}\cdots\text{C}_{ipso}$ (see Table 1 for a

summary of a structure search in the Cambridge Structural Database).

In order to generalize the preference of the heterometals for one of these supplementary interactions and the stabilization that they provide, we have calculated DFT, HF, and MP2 on different model systems. First, we have fully optimized the $[\text{AuR}_2]^-$ ($\text{R} = \text{C}_6\text{F}_5$, $\text{C}_6\text{F}_3\text{Cl}_2$ and C_6Cl_5) basic units by using a D_{2h} symmetry at MP2 level. Then, in order to check the basicity of the different aurates, we have evaluated the interaction energy between these aurate units and one Ag^+ cation using models with C_{2v} symmetry at HF and MP2 levels. We have checked both the ionic and dispersive components of the metallophilicity for these C_{2v} models, depending on the perhalophenyl rings bonded to gold(I) at different interaction distances. Once the basicity of the aurates has been established and taking into account that the main component of the interaction is ionic, we have also fully optimized at DFT level the dinuclear $[\text{AuR}_2]^- \cdots \text{M}^+$ systems allowing the M^+ ($\text{M} = \text{Ag}$, Cu and Ti) centers to interact both with the C_{ipso} (C_s symmetry) or the X_{ortho} atoms of the perhalophenyl rings (C_2 symmetry). The computed bsse(basis set superposition error)-corrected MP2 interaction energies of these DFT-optimized models permit to check the preference of the heterometal for a weak interaction additional to the metallophilicity and compare it with the experimental results (see Fig. 1).

2 Methodology

All calculations were made using the Gaussian 03 package program [34]. The molecular geometries of model systems

Scheme 1 Representative examples of heterometallic $\text{Au}\cdots\text{M}$ complexes built up through the interaction between aurates and Lewis acid metal centers such us $\text{Ag}(\text{I})$, $\text{Cu}(\text{I})$, and $\text{Ti}(\text{I})$

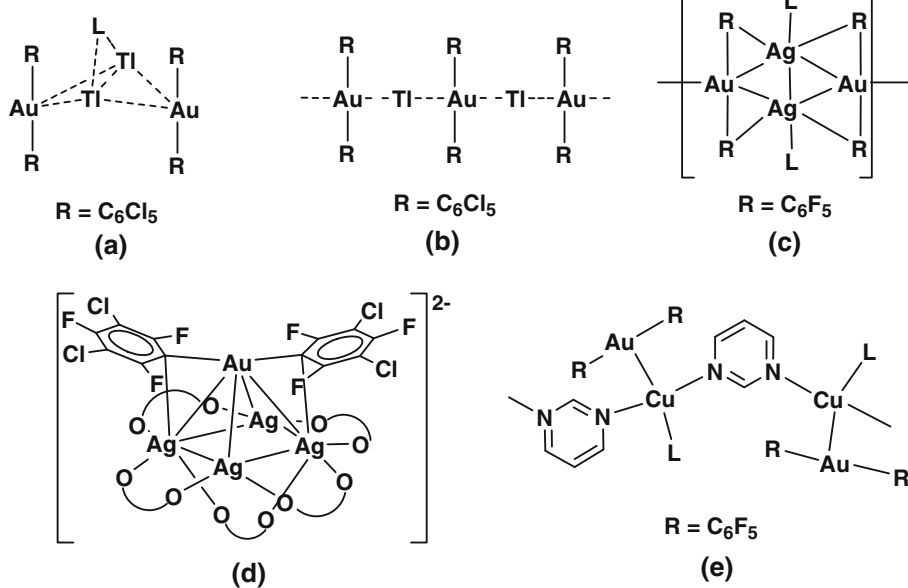


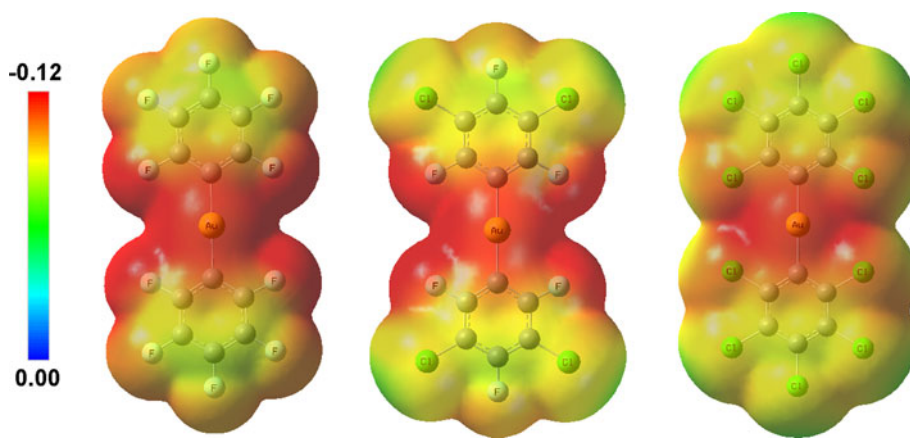
Table 1 Interaction distances between aurates and Ag(I), Cu(I), or Tl(I) closed-shell centers obtained from the Cambridge Structural Database

Compound	Au···M	M···C _{ipso}	M···X	CCDC ref	Reference
[Au ₂ Ag ₂ (C ₆ F ₅) ₄ (thf) ₂] _n	2.717	2.803	—	BAJME	[22]
[Au ₂ Ag ₂ (C ₆ F ₅) ₄ (C ₆ H ₆) ₂] _n	2.792	3.408	—	CEGSOW	[23]
[Au ₂ Ag ₂ (C ₆ F ₅) ₄ (Me ₂ CO) ₂] _n	2.783, 2.791	2.440	—	EBIGAX	[8]
[Au ₂ Ag ₂ (C ₆ F ₅) ₄ (thf) ₂] _n	2.771, 2.758	2.467	—	EGOHIX	[9]
[Au ₂ Ag ₂ (C ₆ F ₅) ₄ (MeCN) ₂] _n	2.758, 2.827	2.687	—	VENWOB	[10]
[AuAg ₄ (C ₆ F ₃ Cl ₂) ₂ (CF ₃ CO ₂) ₅] ²⁻	3.013–2.902	2.450, 2.439	—	XALWUD	[20]
[AuCu(C ₆ F ₅) ₂ (MeCN)(Pyrim)] _n	2.821	2.628	—	RAQFIZ	[11]
[Au ₂ Cu ₂ (C ₆ F ₅) ₄ (MeCN) ₂] _n	2.574	2.142	—	VENWUH	[10]
[AuCu(C ₆ F ₅) ₂ (MeCN) ₂] _n	2.933	2.913	—	—	[12]
[Au ₂ Cu ₂ (C ₆ F ₅) ₄ (PhCN) ₄]	2.616–2.609	2.723, 2.706	—	—	[12]
[AuCu(C ₆ F ₅) ₂ (MeCN) ₂] _n	2.672	2.638	—	—	[12]
[Au ₂ Tl ₂ (C ₆ Cl ₅) ₄ (4,4'-bipy)] _n	3.056	—	3.317, 3.484	AZUDUU	[24]
[Au ₂ Tl ₂ (C ₆ Cl ₅) ₄ (4,4'-bipy) ₂] _n	2.964	—	3.438, 3.547	AZUFAC	[24]
[Au ₄ Tl ₄ (C ₆ Cl ₅) ₈ (4,4'-bipy) ₃] _n	3.122	—	3.448–3.685	AZUFEG	[24]
[Au ₂ Tl ₂ (C ₆ Cl ₅) ₄ (4,4'-bipy) ₂] _n	3.111	—	3.527–3.689	AZUFIK	[24]
[AuTl(C ₆ Cl ₅) ₂ (thf) ₂] _n	3.076	—	3.362	BEXFUG	[25]
[AuTl(C ₆ Cl ₅) ₂ (acacH) ₂] _n	2.969	—	3.652, 3.658	BEXGAN	[25]
[Au ₂ Tl ₂ (C ₆ Cl ₅) ₄ (thf)] _n	2.908	—	3.351, 3.623	BEXGER	[25]
[Au ₂ Tl ₂ (C ₆ Cl ₅) ₄ (Me ₂ CO)]	3.033, 3.188	—	3.297–3.492	EFOWOL	[15]
[AuTl(C ₆ F ₅) ₂ (1,10-phen)] _n	3.082, 3.140	—	2.898	FENKAL	[26]
[AuTl(C ₆ F ₅) ₂ (2,2'-bipy)] _n	3.012, 3.490	—	2.875	FENKEP	[26]
[AuTl(C ₆ F ₅) ₂ (4,4'-bipy)(thf)] _n	3.215, 3.480	—	—	FENKIT	[26]
[Au ₂ Tl ₂ (C ₆ F ₅) ₄ (4,4'-bipy)] _n	3.016	3.517	—	IFECAZ	[27]
[Au ₄ Tl ₄ (C ₆ Cl ₅) ₈ (4,4'-bipy) ₃ (thf) ₂] _n	3.032, 3.054	—	3.549, 3.556	IFECEB	[27]
[Au ₂ Tl ₂ (C ₆ Cl ₅) ₄ (toluene)2(1,4-diox)]	2.893	3.447	3.577	ILIFYOR	[28]
[AuTl(C ₆ F ₅) ₂ (OPPh ₃) ₂] _n	3.036, 3.086	—	3.402, 3.405	JOWYEZ	[29]
{[NBu ₄] ₂ [Au ₆ Tl ₄ (C ₆ Cl ₅) ₁₂]} _n	3.056–3.168	3.510	3.542	KAKGAF	[30]
{[NBu ₄] ₂ [Au ₄ Tl ₂ (C ₆ F ₃ Cl ₂) ₈]} _n	2.970–3–120	3.552	2.924–3.239	KAKGEJ	[30]
{[NBu ₄] ₂ [Au ₄ Tl ₂ (C ₆ Cl ₅) ₄ (C ₆ F ₃ Cl ₂) ₄]} _n	3.011–3.091	3.557	2.916–3.48	KAKGIN	[30]
[Au ₂ Tl ₂ (C ₆ Cl ₅) ₄ (OPPh ₃) ₂ (thf)] _n	3.053–3.163	3.463	3.391–3.638	RUWTOS	[13]
[Au ₂ Tl ₂ (C ₆ Cl ₅) ₄ (OPPh ₃) ₂ (Me ₂ CO)] _n	3.094–3.245	—	3.370–3.444	RUWTUY	[14]
[AuTl(C ₆ Cl ₅) ₂ (toluene)]	2.911	3.519–3.562	3.332–3.365	SICLAS	[31]
[Au ₂ Tl ₂ (C ₆ F ₅) ₄ (DMSO) ₃] _n	3.222–3.246	—	2.864–3.383	TAXZEY	[32]
[Au ₄ Tl ₄ (C ₆ Cl ₅) ₈ (DMSO) ₄] _n	3.122–3.284	—	3.227–3.708	TAXZIC	[32]
[Au ₄ Tl ₄ (C ₆ Cl ₅) ₈ (ⁱ Pr-en) ₄] _n	2.973–3.026	—	3.634	TEGTOP	[16]
[Au ₂ Tl ₂ (C ₆ Cl ₅) ₄ (2- ⁱ Pr-en) ₂] _n	3.052, 3.088	3.575–3.600	3.654	TEDTUV	[16]
[Au ₂ Tl ₂ (C ₆ F ₅) ₄ (2- ⁱ Pr-en) ₂] _n	3.045, 3.143	3.587	3.404	TEGVAD	[16]
[AuTl(C ₆ Cl ₅) ₂] _n	2.973, 3.004	—	3.244, 3.350	TUVMUS	[14]
{[NBu ₄] ₂ [Au ₃ Tl ₂ (C ₆ F ₄ Br) ₆]} _n	3.035–3.125	—	3.013–3.392	VOFBEI	[17]
{[NBu ₄] ₂ [Au ₆ Tl ₄ (C ₆ F ₄ Br) ₁₂]} _n	2.996–3.466	3.541	2.933–3.643	VOFBIC	[17]
{[NBu ₄] ₂ [Au ₄ Tl ₂ (C ₆ F ₄ Br) ₈]} _n	2.935–3.021	3.485	3.231–3.735	VOFBOI	[17]
[Au ₂ Tl ₂ (C ₆ Cl ₅) ₄ (MePhCO)]	3.017–3.231	—	3.243–3.440	WATHIJ	[33]
[Au ₂ Tl ₂ (C ₆ Cl ₅) ₄ (acacH)]	3.085–3.133	—	3.168–3.525	WATHOP	[33]
[Au ₂ Tl ₂ (C ₆ Cl ₅) ₄ (acacH)(4,4'-bipy)]	3.031	—	3.241	WATHUV	[33]

[Au(C₆F₅)₂]⁻, [Au(C₆F₃Cl₂)₂]⁻, and [Au(C₆Cl₅)₂]⁻ were fully optimized at MP2 level of theory using a D_{2h} symmetry. Electronic correlation effects, keeping the core

orbitals frozen, were also included in further single point calculations on model systems [AuR₂]⁻···Ag⁺ (R = C₆F₅, C₆F₃Cl₂ and C₆Cl₅) at various Au–Ag distances by using

Fig. 1 Electron density maps from total MP2 density (isoval = 0.02; mapped with electrostatic potential (ESP)) for model systems $[\text{AuR}_2]^-$ ($\text{R} = \text{C}_6\text{F}_5$, $\text{C}_6\text{F}_3\text{Cl}_2$, and C_6Cl_5)



second-order Møller-Plesset perturbation theory or Hartree-Fock calculations. The interaction energy at Hartree-Fock (HF) and MP2 levels of theory was obtained according to Eq. 1:

$$\Delta E = E_{AB}^{(AB)} - E_A^{(AB)} - E_B^{(AB)} = V(R) \quad (1)$$

A counterpoise correction for the basis set superposition error (bsse) [35] on ΔE was thereby performed, where $E_{AB}^{(AB)}$ is the total energy of the dimer AB (A = aurate unit, $B = \text{M}^+$ heterometal) calculated with the full basis set AB of the dimer; $E_A^{(AB)}$ and $E_B^{(AB)}$ denote the total energies of monomers A and B , respectively, computed with the dimer basis set AB , i.e., in the calculation of monomer A the basis set of the “other” monomer B is present at the same location as in dimer A , but the nuclei of B are not. In this way, the basis set for each monomer is extended by the functions of the other monomer. The optimized interaction energies (ΔE) and $\text{Au}\cdots\text{M}$ distances for models $[\text{AuR}_2]^- \cdots \text{Ag}^+$ ($\text{R} = \text{C}_6\text{F}_5$, $\text{C}_6\text{F}_3\text{Cl}_2$ and C_6Cl_5) have been estimated. We fitted the calculated points using the four-parameter Eq. 2, which had been previously used to derive the Herschbach-Laurie relation (see Fig. 2) [36]:

$$\Delta E = V(R) = Ae^{-BR} - CR^{-n} \quad (2)$$

The additional stabilization produced by the interaction of the heterometals with the C *ipso* or with the halogen atoms in *ortho* position of the perhalophenyl rings has been studied through the full BSSE-corrected MP2 calculation of DFT-B3LYP-optimized models $[\text{AuR}_2]^- \cdots \text{Ag}^+$ ($\text{R} = \text{C}_6\text{Cl}_5$ and C_6F_5); $[\text{AuR}_2]^- \cdots \text{Cu}^+$ ($\text{R} = \text{C}_6\text{F}_5$ and C_6Cl_5) and $[\text{AuR}_2]^- \cdots \text{Ti}^+$ ($\text{R} = \text{C}_6\text{Cl}_5$ and C_6F_5) with a C_{2v} , C_2 , and C_s symmetries.

The following basis set combination was employed: for the metals, the 19-VE or 21-VE pseudopotentials from Stuttgart and the corresponding basis sets [37] augmented with two f polarization functions were used [38]; the atoms C, Cl, and F were treated by Stuttgart pseudopotentials [39], including only the valence electrons for each atom.

For these atoms, double-zeta basis sets of reference [39] were used, augmented by d-type polarization functions [40].

3 Results and Discussion

We have started this study with the full optimization of the anionic model units $[\text{AuR}_2]^-$ ($\text{R} = \text{C}_6\text{F}_5$, $\text{C}_6\text{F}_3\text{Cl}_2$, and C_6Cl_5) at MP2 level of theory. The most important theoretical structural parameters appear in Table 2. These results are close to the experimental ones [41]. The electron density from total MP2 density mapped with the electrostatic potential (ESP) displays the charge distribution on each aurate unit what gives a qualitative idea of the potential interacting sites, taking into account a pure ionic contribution. Also, the NBO analysis on the three models displays the partial charges on the atoms (see Table 3). Thus, both the Au(I), C_{ipso} or X_{ortho} display the largest amount of electron density at the corresponding models, making these parts of the molecules potential links to the heterometals (see Fig. 1). In particular, when $\text{R} = \text{C}_6\text{F}_5$ or $\text{C}_6\text{F}_3\text{Cl}_2$, the electron density is mostly located at the C_{ipso} and the F atoms of the perhalophenyl rings, while for the case of C_6Cl_5 , the electron density is not located at the C_{ipso} and is distributed along all the Cl atoms at the ring. This NBO analysis already points out a preference of $\text{M}\cdots\text{Cl}_{ortho}$

Table 2 Most important optimized structural distances (\AA) for models $[\text{AuR}_2]^-$ ($\text{R} = \text{C}_6\text{F}_5$ **A**, $\text{C}_6\text{F}_3\text{Cl}_2$ **B**, and C_6Cl_5 **C**) at MP2 level of theory in D_{2h} symmetry

	$[\text{Au}(\text{C}_6\text{F}_5)_2]^-$	$[\text{Au}(\text{C}_6\text{F}_3\text{Cl}_2)_2]^-$	$[\text{Au}(\text{C}_6\text{Cl}_5)_2]^-$
$\text{Au}-\text{C}_{ipso}$	2.025	2.025	2.027
$\text{C}-\text{X}_{ortho}$	1.346	1.343 (F)	1.749
$\text{C}-\text{X}_{meta}$	1.344	1.740 (Cl)	1.742
$\text{C}-\text{X}_{para}$	1.340	1.338 (F)	1.739

Table 3 Most important NBO charges for $[\text{AuR}_2]^-$ models ($\text{R} = \text{C}_6\text{F}_5$ **A**, $\text{C}_6\text{F}_3\text{Cl}_2$ **B**, and C_6Cl_5 **C**) at MP2 level of theory in D_{2h} symmetry

	$[\text{Au}(\text{C}_6\text{F}_5)_2]^-$	$[\text{Au}(\text{C}_6\text{F}_3\text{Cl}_2)_2]^-$	$[\text{Au}(\text{C}_6\text{Cl}_5)_2]^-$
Au	0.363	0.364	0.072
C_{ipso}	-0.500	-0.519	-0.034
X_{ortho}	-0.415	-0.411	-0.247
X_{meta}	-0.414	-0.012	-0.224
X_{para}	-0.412	-0.409	-0.215

interaction when $\text{R} = \text{C}_6\text{Cl}_5$ and both possibilities when $\text{R} = \text{C}_6\text{F}_5$ or $\text{C}_6\text{F}_3\text{Cl}_2$ (Table 3).

Since the possible interaction of the acidic closed-shell metal centers (M^+) with the Au(I) centers would have an ionic and a dispersive component, we have analyzed the interaction between the basic aurate units and silver(I) using the HF and MP2 level of theory, which account for the ionic component of the interaction in the HF case and for the ionic and the dispersive component in the MP2 one.

The analysis of the pure $\text{Au}\cdots\text{Ag}$ interaction by changing the perhalophenyl rings (C_6F_5 , $\text{C}_6\text{F}_3\text{Cl}_2$ and C_6Cl_5) is represented in Fig. 2. The basicity of the three different aurate units has been analyzed at HF and MP2 levels of theory in the model systems $[\text{AuR}_2]^- \cdots \text{Ag}^+$ ($\text{R} = \text{C}_6\text{F}_5$, $\text{C}_6\text{F}_3\text{Cl}_2$ and C_6Cl_5). We have observed that the $\text{Au}\cdots\text{Ag}$ equilibrium distances obtained at HF level is 2.70 Å in all cases, showing a slightly larger stabilization for the model with C_6Cl_5 ligands (-391 kJ mol^{-1}) when compared with the $\text{C}_6\text{F}_3\text{Cl}_2$ (-388 kJ mol^{-1}) and C_6F_5 ligands (-386 kJ mol^{-1}). In any case, the obtained ionic stabilization is already very important for the three models, the bis(pentachlorophenyl)aurate unit being the most basic gold anion. When correlation effects are included an additional stabilization assigned to dispersion for the intermetallic interaction is achieved with the values depending on the perhalophenyl ligand: C_6Cl_5 (-496 kJ mol^{-1}), $\text{C}_6\text{F}_3\text{Cl}_2$ (-485 kJ mol^{-1}), and C_6F_5 (-491 kJ mol^{-1}). The difference between the interaction energy at MP2 and HF levels gives the dispersion component of the interaction: C_6Cl_5 (-105 kJ mol^{-1}), $\text{C}_6\text{F}_3\text{Cl}_2$ (-97 kJ mol^{-1}), and C_6F_5 (-104 kJ mol^{-1}).

As a conclusion of this set of calculations, the analysis of the HF and MP2 curves shows that the basicity of the aurates is not very different, but it is slightly larger for the pentachlorophenyl-substituted aurate, since the Cl atoms are less electronegative than the F ones and more electron density is available from the aurate unit. This trend is already observed at HF level when correlation effects are not included. The use of MP2 accounts for the dispersive component of the interaction giving rise to results that are consistent with previously calculated ones and showing an

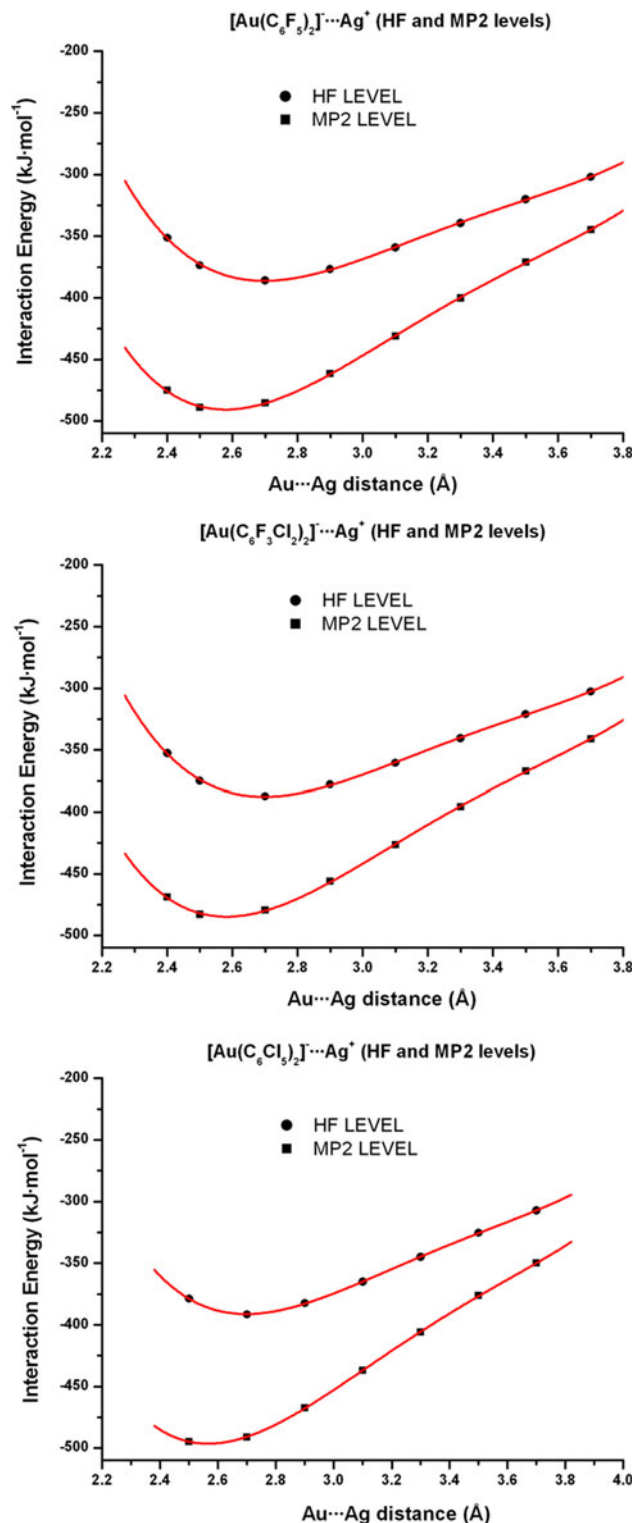


Fig. 2 Interaction energy curves at HF and MP2 levels of theory for model systems $[\text{AuR}_2]^- \cdots \text{Ag}^+$ ($\text{R} = \text{C}_6\text{F}_5$, $\text{C}_6\text{F}_3\text{Cl}_2$, and C_6Cl_5)

ionic character of around 80% and a dispersive component of ca. 20% of the interaction energies. It is worth mentioning that the obtained equilibrium distances are shorter,

and the interaction energies larger than in similar systems previously studied. In this study, we are not considering the presence of ligands attached to the heterometals in order to save computational cost and we let a pure positive charge on the different heterometals (Ag, Cu, or Tl) interacting with the aurate units. From an electronic point of view, the “naked” metal ions have a pure +1 charge what would give rise to a stronger ionic interaction with the aurate units. Moreover, the absence of ligands bonded to M^+ ions would give rise to a less steric hindrance allowing shorter interaction distances. The results will be valid for comparison between theoretical models and experimental results.

The second type of calculations are DFT-B3LYP optimization of model systems models $[AuR_2]^- \cdots Ag^+$ ($R = C_6Cl_5$, and C_6F_5); $[AuR_2]^- \cdots Cu^+$ ($R = C_6F_5$, and C_6Cl_5); and $[AuR_2]^- \cdots Tl^+$ ($R = C_6F_5$ and C_6Cl_5) with a C_{2v} , C_2 , and C_s symmetries. At this level of theory, we can analyze whether the corresponding symmetries depicted in Fig. 3 give rise to stable situations in all cases or not. We use this level of theory since the ionic component of the interaction is the main contribution and DFT is able to reproduce this type of interaction and mimic the dispersive component to some extent [3]. The bsse-corrected MP2 single point calculations on each optimized model system permit the evaluation of the interaction energies between the aurates and the heterometals. Thus, the difference in energy between the C_{2v} and C_2 symmetries allows us to account for the $M \cdots X_{ortho}$ interaction energy, while the difference between the C_{2v} and the C_s symmetry permits to account for the $M \cdots C_{ipso}$ interaction energy. In the case of $M \cdots X$ interactions, we have used a C_2 model with twisted perhalophenyl rings in the bisperhalophenyl unit. This C_2 model would represent two experimentally observed

situations such as the described C_2 with twisted rings (c) and a different situation of almost coplanar perhalophenyl rings interacting with two different heterometals at each side of the aurate unit through the gold center and the X atoms in ortho position (d). A summary of all analyzed model systems is depicted in Fig. 3.

Table 4 displays the main structural parameters optimized at DFT level and the bsse-corrected interaction energies at HF and MP2 level of theory for the six gold–silver models. The first important result is that, among the studied cases, the C_2 model system $[Au(C_6F_5)_2]^- \cdots Ag^+$ does not converge within this symmetry. This trend is in agreement with the up to date known examples of X-ray diffraction studies of heteronuclear Au–Ag complexes in which the tendency of the silver(I) centers is similar to the one represented in the C_s symmetry that favors a $Ag \cdots C_{ipso}$ interaction (Table 1). The analysis of the interaction energies for the rest of the model systems also gives rise to important results. Regarding the interaction between the aurates and Ag^+ in a C_{2v} symmetry (pure $Au \cdots Ag$ interaction), both analyzed geometries are stabilized by a strong ionic component observed at HF level and an extra stabilization due to dispersive (van der Waals) interactions between the metals at MP2 level. Note that the $Au \cdots Ag$ equilibrium distances and interaction energies obtained for the C_{2v} symmetry by the point-by-point analysis at MP2 level discussed earlier or the full DFT optimization and further single point MP2 energy calculation are very similar: 2.56 Å and -496 kJ mol^{-1} versus 2.60 Å and $-497.5\text{ kJ mol}^{-1}$ for the $[Au(C_6Cl_5)_2]^- \cdots Ag^+$ and 2.58 Å and -491 kJ mol^{-1} versus 2.60 Å and -491 kJ mol^{-1} for the $[Au(C_6F_5)_2]^- \cdots Ag^+$ one. These results validate the analysis of the interaction between the aurates and other closed-metal centers through DFT optimizations.

Fig. 3 Representation of the analyzed model systems in this study: $[AuR_2]^-$ ($R = C_6Cl_5$, $C_6F_3Cl_2$, and C_6F_5) with a D_{2h} symmetry (a); $[AuR_2]^- \cdots Ag^+$ ($R = C_6Cl_5$ and C_6F_5); $[AuR_2]^- \cdots Cu^+$ ($R = C_6F_5$ and C_6Cl_5) and $[AuR_2]^- \cdots Tl^+$ ($R = C_6F_5$ and C_6Cl_5) with a C_{2v} (b), C_2 (c), and C_s (d) symmetries

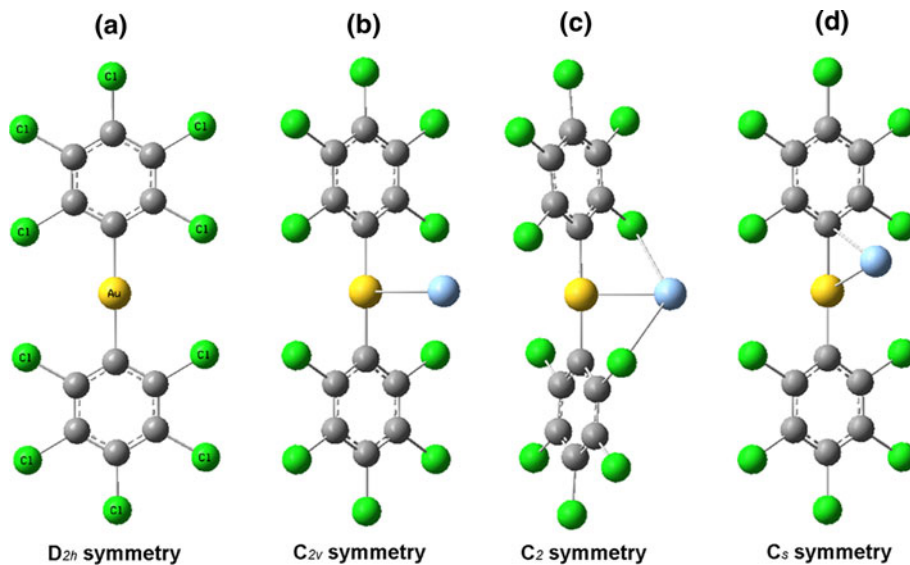


Table 4 DFT-B3LYP-optimized Au···Ag, M···C_{ipso}, and M···X (X = F or Cl) interaction distances (Å) and HF and MP2-BSSE-corrected interaction energies (kJ mol⁻¹) for models [AuR₂]⁻··[Ag]⁺ with C_{2v}, C₂ and C_s symmetries (R = C₆Cl₅, and C₆F₅)

	d(Au···Ag)	d(M···C _{ipso})	d(M···X) (X = Cl or F)	E _{int} (Au···M) (HF) E _{int} (Au···M) (MP2)	E _{int} (M···C _{ipso}) or E _{int} (M···X) (HF and MP2)
[Au(C ₆ Cl ₅) ₂] ⁻ ··[Ag] ⁺ C _{2v}	2.600	—	—	-389 (HF) -497 (MP2)	—
[Au(C ₆ F ₅) ₂] ⁻ ··[Ag] ⁺ C _{2v}	2.596	—	—	-387 (HF) -491 (MP2)	—
[Au(C ₆ Cl ₅) ₂] ⁻ ··[Ag] ⁺ C ₂	2.705	—	2.572	-415 (HF) -549 (MP2)	-26 (HF) -51 (MP2)
[Au(C ₆ F ₅) ₂] ⁻ ··[Ag] ⁺ C ₂	Not converged in C ₂ symmetry				
[Au(C ₆ Cl ₅) ₂] ⁻ ··[Ag] ⁺ C _s	2.666	2.399	—	-403 (HF) -528 (MP2)	-14 (HF) -30 (MP2)
[Au(C ₆ F ₅) ₂] ⁻ ··[Ag] ⁺ C _s	2.681	2.360	—	-404 (HF) -523 (MP2)	-17 (HF) -32 (MP2)

If we have a look at the results for C₂ and C_s symmetries, we obtain slightly larger intermetallic distances than those of the C_{2v} models, but we also detect Ag···Cl interactions in the case of the C₂ [Au(C₆Cl₅)₂]⁻··Ag⁺ model and Ag⁺··C_{ipso} interactions in the C_s [Au(C₆X₅)₂]⁻··Ag⁺ (X = Cl and F) model systems. If we subtract the interaction energy of the Au–Ag model with a C₂ symmetry from the C_{2v} model, we obtain an additional interaction energy of -26 kJ mol⁻¹ at HF level and -51 kJ mol⁻¹ at MP2 level that is due to the interaction between two ortho Cl atoms of the pentachlorophenyl rings with the silver center. Similarly, if we subtract the interaction energy of the [Au(C₆X₅)₂]⁻··Ag⁺ (X = Cl and F) models, with a C_s symmetry, from the corresponding C_{2v} models, we obtain an additional stabilization of -14 kJ mol⁻¹ at HF level and -30 kJ mol⁻¹ at MP2 for the model with pentachlorophenyl ligands and -17 kJ mol⁻¹ at HF level and -30 kJ mol⁻¹ at MP2 for the model with pentafluorophenyl ligands. These additional stabilizations arise from Ag···C_{ipso} interactions for each case. It is worth mentioning that both the Ag···Cl and the Ag···C_{ipso} interactions have an approximately 50% of ionic nature and 50% of dispersion contribution. In view of these results, we can conclude that when pentachlorophenyl ligands are bonded to gold(I), all the studied symmetries are stable, being the C₂ situation (Ag···Cl interactions) more stable than the C_s one (Ag···C_{ipso}). In the case of pentafluorophenyl ligands, although the model bearing Ag···F interactions does not converge to a minimum, the model displaying one Ag···C_{ipso} interaction is -30 kJ mol⁻¹ more stable than the pure Au···Ag interaction. From an experimental point of view, most of the Au···Ag complexes characterized through X-ray diffraction analysis display Ag···C_{ipso} interactions as, for instance, in complexes of the type [Au₂Ag₂(C₆F₅)₄L₂]_n [8–10, 22, 23], in agreement with what we observe theoretically. The theoretical results for [Au(C₆Cl₅)₂]⁻··Ag⁺ model systems can be considered as predictions of plausible structural arrangements since there are no experimental structural results with this ligands bonded to gold.

The same type of analysis has been carried out for the study of the tendency of the acidic Cu⁺ ion in its interaction with the different aurates. The main structural parameters optimized at DFT level and the bsse-corrected interaction energies at HF and MP2 level of theory are given in Table 5. In these cases, we observe that at DFT level, both C₂ model systems [Au(C₆X₅)₂]⁻··Cu⁺ (X = Cl and F) do not converge within this symmetry. Again, this result is in agreement with the already reported examples obtained from the X-ray diffraction studies for Au–Cu complexes. In the same way as for the silver case, the Cu···X interactions are not observed experimentally, and this could be due to the smaller size of the Cu(I) closed-shell center [10–12]. The interaction energies between the aurates and Cu⁺ in a C_{2v} symmetry (pure Au···Cu interaction) are slightly stronger than the above described for the Au···Ag case, but display similar contributions (ca. 80% ionic, 20% dispersion). The optimized Au···Cu interaction distances are also shorter than the Au···Ag cases as it is also observed experimentally.

The results for the Au–Cu models in a C_s symmetry display the expected formation of Au···Cu metallophilic and Cu···C_{ipso} interactions (see Table 5). The optimized intermetallic distances are larger than the ones of the C_{2v} models, leading to theoretically predicted Au–Cu and Cu···C_{ipso} distances, which are comparable with the experimental ones. If we subtract the interaction energy of the Au–Cu models with a C_s symmetry from the corresponding C_{2v} models, we observe that the C_s symmetries are more stable than the C_{2v} ones in -78 kJ mol⁻¹ when R = C₆Cl₅ and -72 kJ mol⁻¹ for R = C₆F₅. This additional stabilization is attributed to the formation of a fairly strong Cu···C_{ipso} interaction. In the Au–Cu case, the Cu···C_{ipso} interactions display a 55% of ionic nature and 45% of dispersion. Therefore, we can conclude that the Cu···X interactions are not favored for this type of molecules, while the Cu···C_{ipso} interactions are very strong. Experimentally, all reported Au–Cu complexes [10–12] display the latter interaction, in agreement with this theoretical analysis (Table 1).

Table 5 DFT-B3LYP-optimized Au···Cu, M···C_{ipso} and M···X (X = F or Cl) interaction distances (\AA) and HF and MP2-BSSE-corrected interaction energies (kJ mol⁻¹) for models [AuR₂]⁻···[Cu]⁺ with C_{2v}, C₂ and C_s symmetries (R = C₆Cl₅, and C₆F₅)

	d(Au···Cu)	d(M···C _{ipso})	d(M···X) (X = Cl or F)	E _{int} (Au···M) (HF) E _{int} (Au···M) (MP2)	E _{int} (M···C _{ipso}) (HF and MP2)
[Au(C ₆ Cl ₅) ₂] ⁻ ···[Cu] ⁺ C _{2v}	2.392	—	—	-424 (HF) -531 (MP2)	—
[Au(C ₆ F ₅) ₂] ⁻ ···[Cu] ⁺ C _{2v}	2.390	—	—	-421 (HF) -524 (MP2)	—
[Au(C ₆ Cl ₅) ₂] ⁻ ···[Cu] ⁺ C ₂	Not converged in C ₂ symmetry				
[Au(C ₆ F ₅) ₂] ⁻ ···[Cu] ⁺ C ₂	Not converged in C ₂ symmetry				
[Au(C ₆ Cl ₅) ₂] ⁻ ···[Cu] ⁺ C _s	2.492	2.015	—	-467 (HF) -609 (MP2)	-43 (HF) -78 (MP2)
[Au(C ₆ F ₅) ₂] ⁻ ···[Cu] ⁺ C _s	2.503	2.011	—	-461 (HF) -596 (MP2)	-39 (HF) -72 (MP2)

The theoretical results clearly change when the studied metallophilic interaction is Au(I)···Tl(I). In this case, the preliminary DFT optimizations of the six model systems reveal the first difference with the Au–Ag and Au–Cu cases. Thus, while in the case of the gold–silver and gold–copper interactions, the convergence problems were found for the C₂ symmetry, in the gold–thallium case, the [Au(C₆F₅)₂]⁻···Tl⁺ model in a C_s symmetry does not converge to a minimum within this symmetry and losses the Tl···C_{ipso} interaction proposed at the starting point of the optimization, leading to a C_{2v} symmetry with a pure metallophilic interaction between charged fragments. Experimentally, among the seven Au–Tl complexes bearing C₆F₅ ligands, only one of them, complex [Au₂Tl]₂(C₆F₅)₄(4,4'-bipy)₂]_n, displays a very weak Tl···C_{ipso} interaction of 3.517 Å [27]. This complex is also special for other reasons as it is the fact that it does not follow the classic Coulomb rules showing a +--+ metal arrangement. All the optimized model systems give rise to short Au···Tl interactions and in the case of C₂ and C_s models additional Tl···X and Tl···C_{ipso} interactions, respectively, except for the model system that does not converge to a minimum. The bsse-corrected MP2 interaction energies for the C_{2v} models show that the Au···Tl interaction is also very strong for these systems with a very important ionic contribution (ca. 80%) and an additional dispersion contribution (ca 20%). These results, although give rise to larger interaction energies due to the absence of ligands bonded to the

heterometals, are in agreement with previously calculated ones in terms of ionic and dispersion percentages [13, 18]. Again, the analysis of the model systems in C₂ or C_s symmetries permits the evaluation of the possible Tl···X_{ortho} and Tl···C_{ipso} interactions, respectively. The interaction energy calculations of the C₂ model systems give rise to a larger stabilization than in the corresponding C_{2v} models (see Table 6). As we have carried out for the former models, if we subtract the interaction energy of the C₂ [Au(C₆Cl₅)₂]⁻···Tl⁺ model from that of the C_{2v} model, we obtain an additional interaction energy of -8.4 kJ mol⁻¹, at HF level and -15.6 kJ mol⁻¹ at MP2 level, which is due to the interaction between two *ortho* Cl atoms of the pentachlorophenyl rings with the thallium center. Similarly, the C₂ [Au(C₆F₅)₂]⁻···Tl⁺ model displays an additional stabilization arising from the Tl···F_{ortho} interactions of -20 kJ mol⁻¹ at HF level and -22 kJ mol⁻¹ at MP2 level. As it can be seen, both the Tl···Cl and Tl···F interactions are possible for this geometry, being the character of the latter almost purely ionic, while the Tl···Cl interaction shows similar ionic and dispersive contributions. If we have a look at the experimentally known Au–Tl complexes in Table 1, only two among 33 complexes do not display a Tl···X interaction.

Regarding the optimized C_s [Au(C₆Cl₅)₂]⁻···Tl⁺ model, the analysis of the additional stabilization arising from a Tl···C_{ipso} interaction shows that it is slightly repulsive at HF level and only attractive by -2 kJ mol⁻¹ at MP2 level. This

Table 6 DFT-B3LYP optimized Au···Tl, M···C_{ipso} and M···X (X = F or Cl) interaction distances (\AA) and HF and MP2-BSSE-corrected interaction energies (kJ mol⁻¹) for models [AuR₂]⁻···[Tl]⁺ with C_{2v}, C₂, and C_s symmetries (R = C₆Cl₅ and C₆F₅)

	d(Au···Tl)	d(M···C _{ipso})	d(M···X) (X = Cl or F)	E _{int} (Au···M) (HF) E _{int} (Au···M) (MP2)	E _{int} (M···C _{ipso}) or E _{int} (M···X) (HF and MP2)
[Au(C ₆ Cl ₅) ₂] ⁻ ···[Tl] ⁺ C _{2v}	2.800	—	—	-344 (HF) -434 (MP2)	—
[Au(C ₆ F ₅) ₂] ⁻ ···[Tl] ⁺ C _{2v}	2.812	—	—	-339 (HF) -422 (MP2)	—
[Au(C ₆ Cl ₅) ₂] ⁻ ···[Tl] ⁺ C ₂	2.858	—	3.345	-352 (HF) -450 (MP2)	-8 (HF) -16 (MP2)
[Au(C ₆ F ₅) ₂] ⁻ ···[Tl] ⁺ C ₂	2.895	—	2.809	-359 (HF) -444 (MP2)	-20 (HF) -22 (MP2)
[Au(C ₆ Cl ₅) ₂] ⁻ ···[Tl] ⁺ C _s	2.812	3.111	—	-343 (HF) -436 (MP2)	+1 (HF) -2 (MP2)
[Au(C ₆ F ₅) ₂] ⁻ ···[Tl] ⁺ C _s	Not converged in C _s symmetry				

result, together with non-converged C_s $[Au(C_6F_5)_2]^- \cdots Tl^+$ case, demonstrates a clear preference of the Tl^+ ions for a C_2 symmetry leading to $Tl \cdots X_{ortho}$ interactions. If we analyze carefully the experimental results, the most common feature of aurate–thallium complexes is the existence of such type of additional $Tl \cdots X$ interactions in the presence or not of $Tl \cdots C_{ipso}$ interactions, in contrast to what we observe for Au–Ag and Au–Cu model systems. Again, the theoretical results show here a good agreement with the experimental ones [13–17, 24–33]. Finally, comparison of these results with calculations with higher correlated methods as CCDS(T) [42] ones are envisaged.

4 Conclusions

Several interesting conclusions can be stated in view of the theoretical analysis of the aurate–heterometal interactions as follows:

1. The basicity of the aurates has been analyzed in their interaction with the silver(I) center as a representative example of closed-shell cation, leading to a basicity order: $[Au(C_6Cl_5)_2]^- > [Au(C_6F_3Cl_2)_2]^- > [Au(C_6F_5)_2]^-$, although with interaction energy values in a similar energy range.
2. The analysis of the Au–Ag systems is in agreement with a preference for $Ag \cdots C_{ipso}$ interaction when $R = C_6F_5$ and $Ag \cdots Cl$ interaction when $R = C_6Cl_5$. In the case of Au–Cu systems, the preference is always the $Cu \cdots C_{ipso}$ interaction even if the perhalophenyl group is C_6Cl_5 , what would be rationalized in terms of atom size.
3. The analysis of the Au–Tl systems displays a clear preference for $Tl \cdots X_{ortho}$ interactions, even in the case of C_6F_5 that does not converge in C_s symmetry ($Tl \cdots C_{ipso}$ interaction) even if the C_{ipso} bears electron density for a possible interaction. This last trend would also be rationalized in terms of atom size, although the change of hybridization in the case of $Tl(I)$ bearing a $6s^2$ lone pair would influence in the electronic requirements of the acidic Tl^+ site.

Acknowledgments The D.G.I.(MEC)/FEDER (CTQ2010-20500-C02-02), European Commission, POCTEFA (MET-NANO EFA 17/08) and CSIC-U. de Chile 02/09-10 projects are acknowledged. We also thank to the Centro de Computación de Galicia (CESGA) for computational resources.

References

1. Laguna A (ed) (2008) Modern supramolecular gold chemistry. Wiley-VCH, Weinheim
2. Pyykkö P (1997) Chem Rev 97:597
3. Pyykkö P (2004) Angew Chem Int Ed 43:4412
4. Pyykkö P (2005) Inorg Chim Acta 358:4113
5. Pyykkö P (2008) Chem Soc Rev 37:1967
6. Fernández EJ, Laguna A, López-de-Luzuriaga JM (2007) Dalton Trans 1969
7. Forward JM, Fackler, JP Jr, Assefa Z (1999) In: Roundhill DM, Fackler JP Jr (eds) Optoelectronic properties of inorganic compounds. Plenum, New York
8. Fernández EJ, Gimeno MC, Laguna A, López-de-Luzuriaga JM, Monge M, Pyykkö P, Sundholm D (2000) J Am Chem Soc 122:7287
9. Fernández EJ, López-de-Luzuriaga JM, Monge M, Olmos ME, Puelles RC, Laguna A, Mohamed AA, Fackler JP Jr (2008) Inorg Chem 47:8069
10. Fernández EJ, Laguna A, López-de-Luzuriaga JM, Monge M, Montiel M, Olmos ME, Rodríguez-Castillo M (2006) Organometallics 26:3639
11. Fernández EJ, Laguna A, López-de-Luzuriaga JM, Monge M, Montiel M, Olmos ME (2005) Inorg Chem 44:1163
12. Fernández EJ, Laguna A, López-de-Luzuriaga JM, Monge M, Montiel M, Olmos ME, Rodríguez-Castillo M (2006) Dalton Trans 2009:7509
13. Fernández EJ, Laguna A, López-de-Luzuriaga JM, Mendizabal F, Monge M, Olmos ME, Pérez J (2003) Chem Eur J 9:456
14. Fernández EJ, López-de-Luzuriaga JM, Monge M, Olmos ME, Pérez J, Laguna A, Mohamed AA, Fackler JP Jr (2003) J Am Chem Soc 125:2022
15. Fernández EJ, Laguna A, López-de-Luzuriaga JM, Monge M, Olmos ME, Pérez J (2002) J Am Chem Soc 124:5942
16. Fernández EJ, Laguna A, López-de-Luzuriaga JM, Montiel M, Olmos ME, Pérez J (2006) Organometallics 25:1689
17. Fernández EJ, Laguna A, Lasanta T, López-de-Luzuriaga JM, Montiel M, Olmos ME (2008) Organometallics 27:2971
18. Fernández EJ, Laguna A, López-de-Luzuriaga JM, Monge M, Mendizabal F (2008) J Mol Struct 851:121
19. Fernández EJ, Laguna A, López-de-Luzuriaga JM, Monge M, Nema M, Olmos ME, Pérez J, Silvestre C (2007) Chem Commun 571
20. Fernández EJ, Laguna A, López-de-Luzuriaga JM, Monge M, Montiel M, Olmos ME, Pérez J, Puelles RC, Sáenz JC (2005) Dalton Trans 1162
21. Fernández EJ, Hardacre C, Laguna A, Lagunas MC, López-de-Luzuriaga JM, Monge M, Montiel M, Olmos ME, Puelles RC, Sánchez-Forcada E (2009) Chem Eur J 15:6222
22. Uson R, Laguna A, Laguna M, Jones PG, Sheldrick GM (1981) J Chem Soc Chem Commun 1097
23. Uson R, Laguna A, Laguna M, Manzano BR, Jones PG, Sheldrick GM (1984) J Chem Soc Dalton Trans 285
24. Fernández EJ, Laguna A, López-de-Luzuriaga JM, Olmos ME, Pérez J (2004) Dalton Trans 1801
25. Fernández EJ, López-de-Luzuriaga JM, Monge M, Montiel M, Olmos ME, Pérez J, Laguna A, Mendizabal F, Mohamed AA, Fackler JP Jr (2004) Inorg Chem 43:3573
26. Fernández EJ, Jones PG, Laguna A, López-de-Luzuriaga JM, Monge M, Montiel M, Olmos ME, Pérez J (2004) Z Naturforsch B 59:1379
27. Fernández EJ, Jones PG, Laguna A, López-de-Luzuriaga JM, Monge M, Pérez J, Olmos ME (2002) Inorg Chem 41:1056
28. Fernández EJ, Laguna A, López-de-Luzuriaga JM, Olmos ME, Pérez J (2003) Chem Commun 1760
29. Crespo O, Fernández EJ, Jones PG, Laguna A, López-de-Luzuriaga JM, Mendía A, Monge M, Olmos E (1998) Chem Commun 2233
30. Fernández EJ, Laguna A, López-de-Luzuriaga JM, Montiel M, Olmos ME, Pérez J (2005) Organometallics 24:1631

31. Fernández EJ, Laguna A, López-de-Luzuriaga JM, Monge M, Montiel M, Olmos ME (2007) Inorg Chem 46:2953
32. Fernández EJ, Laguna A, López-de-Luzuriaga JM, Montiel M, Olmos ME, Pérez J (2005) Inorg Chim Acta 358:4293
33. Fernández EJ, López-de-Luzuriaga JM, Olmos ME, Pérez J, Laguna A, Lagunas MC (2005) Inorg Chem 44:6012
34. Frisch MJ, Trucks GW, Schlegel HB, Scuseria GE, Robb MA, Cheeseman JR, Zakrzewski VG, Montgomery JA Jr, Stratmann RE, Burant JC, Dapprich S, Millam JM, Daniels AD, Kudin KN, Strain MC, Farkas O, Tomasi J, Barone V, Cossi M, Cammi R, Mennucci B, Pomelli C, Adamo C, Clifford S, Ochterski J, Petersson GA, Ayala PY, Cui Q, Morokuma K, Malick DK, Rabuck AD, Raghavachari K, Foresman JB, Cioslowski J, Ortiz JV, Stefanov BB, Liu G, Liashenko A, Piskorz P, Komaromi I, Gomperts R, Martin RL, Fox DJ, Keith T, Al-Laham MA, Peng CY, Nanayakkara A, Gonzalez C, Challacombe M, Gill PMW, Johnson B, Chen W, Wong MW, Andres JL, Gonzalez C, Head-Gordon M, Replogle ES, Pople JA (2004) Gaussian 03, Rev. E. 01. Gaussian Inc, Wallingford
35. Boys SF, Bernardi F (1970) Mol Phys 19:553
36. Herschbach DR, Laurie VW (1961) J Chem Phys 35:458
37. Andrae D, Häusserman U, Dolg M, Stoll H, Preuss H (1990) Theor Chim Acta 77:123
38. Pyykkö P, Runeberg N, Mendizabal F (1997) Chem Eur J 3:1451
39. Bergner A, Dolg M, Küchle W, Stoll H, Preuss H (1993) Mol Phys 80:1431
40. Huzinaga S (1984) Gaussian basis sets for molecular calculations. Elsevier, Amsterdam
41. Fernández EJ, Laguna A, Olmos ME (2009) Coord Chem Rev 252:1630
42. Riedel S, Pyykkö P, Mata RA, Werner HJ (2005) Chem Phys Lett 405:148